Inorganic Chemistry
Article

Inorg. Chem. **2009**, *48*, 6109–6116 **6109**
DOI: 10.1021/ic9004938

Bimetallic Iron(3+) Spin-Crossover Complexes Containing a 2,2′-Bithienyl Bridging bis-QsalH Ligand

Brandon Djukic,[†] Prashanth K. Poddutoori,[†] Paul A. Dube,[§] Takele Seda,[‡] Hilary A. Jenkins,[§] and Martin T. Lemaire*[,†]

[†]*Department of Chemistry, Brock University, St. Catharines, Ontario L2S 3A1, Canada,*
[‡]*Department of Physics and Astronomy, Western Washington University, Bellingham, Washington 98225, and*
[§]*Brockhouse Institute for Materials Research, McMaster University, Hamilton, Ontario L8S 4M1, Canada*

Received March 12, 2009

We describe the synthesis of a new 3,3′-diethynyl-2,2′-bithienyl bridging bis-QsalH ligand (**5**), and the preparation of four bimetallic iron(3+) complexes containing **5** with Cl^- (**6**), SCN^- (**7**), PF_6^- (**8**), and ClO_4^- (**9**) counteranions. We show with variable temperature magnetic susceptibility, Mössbauer, and electron paramagnetic resonance (EPR) spectroscopy that each complex undergoes a spin-crossover in the solid state. In all four complexes, we observe very gradual and incomplete S = 5/2, 5/2 to S = 1/2, 1/2 spin-crossover processes, with three of the four complexes exhibiting nearly identical magnetic properties. We investigated the electronic properties of the complexes by cyclic and differential pulse voltammetry, and attempted electropolymerization reactions with acetonitrile solutions of the complexes, which were not successful. Each complex features a single iron(3+) reduction wave at approximately −0.7 V (versus ferrocene), and the oxidation of the 2,2′-bithienyl substituent occurs at +1.1 V. These materials represent a new structural paradigm for the study of rare bimetallic iron(3+) spin-crossover complexes.

Introduction

Spin-crossover (SCO) in coordination complexes containing iron(2+) or (3+) provides one of the best examples of molecular bistability, said to occur when a molecule can exist from among distinct electronic states at the same temperature.[1] Typically, a spin-crossover complex will feature a high-to-low-spin conversion that is thermally induced, but SCO can also be effected by light irradiation (LIESST effect) or even upon molecular encapsulation of the paramagnetic complex.[2−5] Often, and in particular with iron(3+) complexes, these transitions are very gradual, but in some special cases the conversion can become abrupt, and thermal hysteresis is observed.[6−8]

By far, the majority of reported SCO complexes contain a single metal ion; however, recently there has been a great deal of interest in the preparation of bi- or polymetallic spin-crossover complexes. These efforts not only enhance our understanding of SCO in polymetallic systems, but also provide a general class of new *multifunctional* materials, including complexes that feature both spin-crossover and magnetic exchange coupling.[9−13] This research, pioneered by Real, Kahn, Murray, Gütlich, Brooker, and Kaizaki has focused on the preparation of bimetallic iron(2+) SCO assemblies, which include a wide variety of typically *N*-heterocyclic bridging ligands, such as 2,2′-bipyrimidine,[14−17] pyridine,[18] pyrazole,[19]

*To whom correspondence should be addressed. E-mail: mlemaire@brocku.ca.

(1) Kahn, O.; Martinez, C. J. *Science* **1998**, *279*, 44–48.
(2) Hayami, S.; Gu, Z.-z.; Shiro, M.; Einaga, Y.; Fujishima, A.; Sato, O. *J. Am. Chem. Soc.* **2000**, *122*, 7126–7127.
(3) Sato, O. *Acc. Chem. Res.* **2003**, *36*, 692–700.
(4) Halcrow, M. A. *Chem. Soc. Rev.* **2008**, *37*, 278–289.
(5) Ono, K.; Yoshizawa, M.; Akita, M.; Kato, T.; Tsunobuchi, Y.; Ohkoshi, S.-i.; Fujita, M. *J. Am. Chem. Soc.* **2009**, *131*, 2782–2783.
(6) Oshio, H.; Kitazaki, K.; Mishiro, J.; Kato, N.; Maeda, Y.; Takashima, Y. *J. Chem. Soc., Dalton Trans.* **1987**, 1341–1347.
(7) Hayami, S.; Gu, Z.-z.; Yoshiki, H.; Fujishima, A.; Sato, O. *J. Am. Chem. Soc.* **2001**, *123*, 11644–11650.
(8) Hayami, S.; Kawahara, T.; Juhasz, G.; Kawamura, K.; Uehashi, K.; Sato, O.; Maeda, Y. *J. Radioanal. Nucl. Ch.* **2003**, *255*, 443–447.
(9) Zein, S.; Borshch, S. A. *J. Am. Chem. Soc.* **2005**, *127*, 16197–16201.
(10) Nihei, M.; Ui, M.; Yokota, M.; Han, L.; Maeda, A.; Kishida, H.; Okamoto, H.; Oshio, H. *Angew. Chem., Int. Ed.* **2005**, *44*, 6484–6487.
(11) Bousseksou, A.; Molnar, G.; Real, J. A.; Tanaka, K. *Coord. Chem. Rev.* **2007**, *251*, 1822–1833.
(12) Murray, K. S. *Eur. J. Inorg. Chem.* **2008**, 3101–3121.
(13) Wu, D.-Y.; Sato, O.; Einaga, Y.; Duan, C.-Y. *Angew. Chem., Int. Ed.* **2009**, *48*, 1475–1478.
(14) Real, J. A.; Zarembowitch, J.; Kahn, O.; Solans, X. *Inorg. Chem.* **1987**, *26*, 2939–2943.
(15) Real, J. A.; Bolvin, H.; Bousseksou, A.; Dworkin, A.; Kahn, O.; Varret, F.; Zarembowitch, J. *J. Am. Chem. Soc.* **1992**, *114*, 4650–4658.
(16) Real, J. A.; Castro, I.; Bousseksou, A.; Verdaguer, M.; Burriel, R.; Castro, M.; Linares, J.; Varret, F. *Inorg. Chem.* **1997**, *36*, 455–464.
(17) Letard, J.-F.; Real, J. A.; Moliner, N.; Gaspar, A. B.; Capes, L.; Cador, O.; Kahn, O. *J. Am. Chem. Soc.* **1999**, *121*, 10630–10631.
(18) Amoore, J. J. M.; Kepert, C. J.; Cashion, J. D.; Moubaraki, B.; Neville, S. M.; Murray, K. S. *Chem. Eur. J.* **2006**, *12*, 8220–8227.
(19) Yoneda, K.; Adachi, K.; Hayami, S.; Maeda, Y.; KatadaM.; Fuyuhiro, A.; Kawata, S.; Kaizaki, S. *Chem. Commun.* **2006**, 45–47.

Published on Web 05/11/2009

triazole,[20,21] bithiazoline,[22] and 4,7-phenanthroline-5,6-diamine[23] derivatives. A number of recent excellent review articles focused completely, or in part, on the structures and properties of bimetallic iron(2+) SCO complexes are available.[11,12]

When compared with the number of published bimetallic iron(2+) SCO complexes, there are far fewer reported examples of their bimetallic iron(3+) counterparts, although both iron(2+) and (3+) bimetallic SCO materials were first reported at nearly the same time. In fact, to our knowledge, the only reported examples of bimetallic iron(3+) SCO complexes typically feature two iron(3+) ions coordinated by pentadentate H_2salten ligands (or simple derivatives of H_2salten, containing other substituents on the salicylaldime rings, particularly methyl or methoxy groups), with the metal centers linked together by different ligand bridges, including pyrazine, 4,4′-bipyridine (or other derivatives of 4,4′-bipyridine, containing unsaturated and saturated bridges between each pyridine ring), or other heterocycles (Figure 1).[24] For instance, the first bimetallic iron(3+) SCO complexes were reported by Ohyoshi, over 20 years ago, and featured two salten^{2-}-coordinated iron(3+) ions linked together with pyrazine, 4,4′-bipyridine, or other bridging ligands.[25] Variable temperature magnetic susceptibility experiments indicated that spin conversion in some of these materials is gradual, and without steps, which suggests that the formation of stable HS-LS intermediate species does not occur in these particular bimetallic complexes. Boča has reported structurally similar bimetallic SCO complexes, with similar magnetic properties.[26] In 2005, Matsumoto reported an unusual bimetallic SCO complex, which exhibited an incomplete, two-step and gradual spin-crossover.[27] Of particular note, X-ray diffraction experiments at 125 K indicated the presence of both high-spin and low-spin iron(3+) within the same complex. Matsumoto has also recently reported another two-step SCO in a bimetallic iron(3+) complex containing a bridging 1,4-bisimidazolylbutane ligand.[28] Unlike their iron(2+) analogues, there are no reported bimetallic iron(3+) SCO complexes that exhibit thermal hysteresis in their magnetic properties, or other LIESST properties.

We have recently reported the synthesis of monometallic iron(3+) SCO complexes containing a thienyl-substituted QsalH ligand (QsalH = *N*-(8-quinolyl)salicylaldimine), as precursors to spin-crossover metallopolymers.[29] As a logical extension of our thienyl-substituted SCO complexes, we thought it would be interesting to design a bridging bis-QsalH ligand containing a 2,2′-bithienyl linker, and to generate a new series of bimetallic iron(3+) SCO complexes. Herein we report the synthesis and characterization of a new bridging bis-QsalH ligand [BT(QsalH)$_2$], and four bimetallic iron(3+) complexes featuring different counteranions (Cl, SCN, PF_6, and ClO_4). In all cases we observe gradual, incomplete SCO from the results of variable temperature magnetic susceptibility and Mössbauer experiments, with similar data for all complexes but the ClO_4, which behaves differently. These complexes represent the first QsalH-type bimetallic SCO materials, and represent a new structural paradigm for the study of SCO in bimetallic iron(3+) complexes.

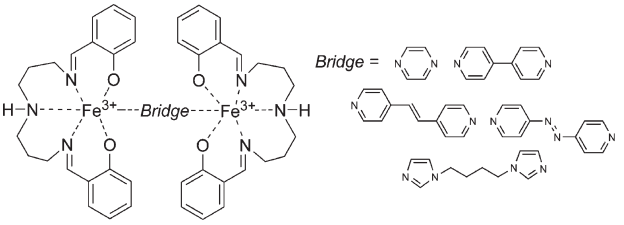

Figure 1. Structures of selected bimetallic SCO complexes (the pentadentate ligand coordinating Fe^{3+} is salten^{2-}).

Experimental Section

General Procedures. All reagents were commercially available and used as received unless otherwise stated. Deaerated and anhydrous solvents were obtained from a Puresolve PS MD-4 solvent purification system, and all air and/or moisture sensitive reactions were carried out using standard Schlenk techniques, unless otherwise stated. $^1H/^{13}C$ NMR spectra were recorded on a Bruker Advance 300 MHz spectrometer with a 7.05 T Ultrashield magnet using deuterated solvents. FT-IR spectra were recorded on a ThermoMattson RS-1 spectrometer as KBr discs or thin films on NaCl plates. EI and FAB mass spectra were obtained using a Kratos Concept 1S High Resolution E/B mass spectrometer; MALDI-TOF mass spectra were obtained using a Bruker Autoflex TOF/TOF MALDI spectrometer. Elemental analyses were carried out by Guelph Chemical Laboratories LTD, Guelph, ON, Canada.

Electrochemical Measurements. Cyclic voltammetry (CV) and differential pulse voltammetry (DPV) experiments were performed with a Bioanalytical Systems Inc. Epsilon electrochemical workstation. Compounds were dissolved in anhydrous solvent (CH_3CN), filtered, and then deareated by sparging with dinitrogen gas for 20 min. Solution concentrations were approximately 10^{-3} M in analyte (depending on solubility) containing 0.1 M supporting electrolyte (Et_4NPF_6). A typical three-electrode setup was used including a platinum working electrode, Ag wire pseudoreference electrode, and a platinum wire auxiliary electrode. Ferrocene was used in all cases as an internal standard and was oxidized at a potential of +0.59 V in our set up; all potentials quoted are versus the ferrocene oxidation potential. Pulse amplitude of 50 mV, pulse width of 50 ms, and pulse period of 100 ms were applied in all DPV experiments. Scan rates for CV and DPV experiments were 100 and 40 mV/s, respectively.

X-ray Structure Determination. Crystals of suitable size were mounted on a glass fiber. Data were collected at room temperature (295 K) on a SMART APEX II diffractometer with Mo Kα radiation (λ = 0.71073 Å) located at the McMaster Analytical X-ray Diffraction Facility (MAX). Data were processed using APEX v2.2.0 and solved by direct methods (SHELXS-97).

Variable Temperature Magnetic Susceptibility Measurements and EPR Spectroscopy. Variable temperature magnetic susceptibility measurements were recorded on

(20) Klingele, M. H.; Moubaraki, B.; Cashion, J. D.; Murray, K. S.; Brooker, S. *Chem. Commun.* **2005**, 987–989.
(21) Grunert, C. M.; Reiman, S.; Spiering, H.; Kitchen, J. A.; Brooker, S.; Gütlich, P. *Angew. Chem., Int. Ed.* **2008**, *47*, 2997–2999.
(22) Ksenofontov, V.; Gaspar, A. B.; Niel, V.; Reiman, S.; Real, J. A.; Gütlich, P. *Chem.—Eur. J.* **2004**, *10*, 1291–1298.
(23) Gaspar, A. B.; Ksenofontov, V.; Reiman, S.; Gütlich, P.; Thompson, A. L.; Goeta, A. E.; Muñoz, M. C.; Real, J. A. *Chem. Eur. J.* **2006**, *12*, 9289–9298.
(24) Nihei, M.; Shiga, T.; Maeda, Y.; Oshio, H. *Coord. Chem. Rev.* **2007**, *251*, 2606–2621.
(25) Ohta, S.; Yoshimura, C.; Matsumoto, N.; Okawa, H.; Ohyoshi, A. *Bull. Chem. Soc. Jpn.* **1986**, *59*, 155–159.
(26) Boča, R.; Fukuda, Y.; Gembický, M.; Herchel, R.; Jaroščiak, R.; Linert, W.; Renz, F.; Yuzurihara, J. *Chem. Phys. Lett.* **2000**, *325*, 411–419.
(27) Kitashima, R.; Imatomi, S.; Yamada, M.; Matsumoto, N.; Maeda, Y. *Chem. Lett.* **2005**, *34*, 1388–1389.
(28) Imatomi, S.; Sato, T.; Hamamatsu, T.; Kitashima, R.; Matsumoto, N. *Bull. Chem. Soc. Jpn.* **2007**, *80*, 2375–2377.
(29) Djukic, B.; Dube, P. A.; Razavi, F.; Seda, T.; Jenkins, H. A.; Britten, J. F.; Lemaire, M. T. *Inorg. Chem.* **2009**, *48*, 699–707.

a superconducting quantum interference device (SQUID) magnetometer (Quantum Design MPMS) with a 5.5 T magnet (temperature range 1.8 to 400 K) in an external field of 5000 Oe. Samples were carefully weighed into polycarbonate capsules, with empty polycarbonate capsules above and below to eliminate background contributions from the capsule, which were loaded into plastic straws, and attached to the sample transport rod. Diamagnetic corrections were made using Pascal's constants. EPR spectra were recorded as powders in quartz tubes on a BrukerElexsys E580 pulsed and CW X-band (9 GHz) spectrometer, equipped with a liquid helium cryostat.

Mössbauer Spectroscopy. Mössbauer spectra were recorded with a constant-acceleration spectrometer (Wissel GMBH, Germany) in a horizontal transmission mode using a 50 mCi ^{57}Co source. A Janis SHI-850-1 closed cycle helium refrigerator cryostat was used for variable temperature measurements. All spectra were fitted by Lorentzian line shapes using NORMOS (Wissel GMBH) least-squares fitting program. The velocity scale was normalized with respect to metallic iron at room temperature; hence, all isomer shifts were recorded relative to metallic iron.

Synthesis

3,3′-Bis(trimethylsilylethynyl)-2,2′-bithiophene (1). 3,3′-Dibromo-2,2′-bithiophene (2.405 g, 7.4 mmol), PPh_3 (0.117 g, 6 mol %), $Pd(PPh_3)_2Cl_2$ (0.312 g, 6 mol %), and CuI (0.085 g, 6 mol %) were combined with 50 mL of deareated anhydrous diisopropylamine. Ethynyltrimethylsilane (3.21 mL, 2.23 g, 22.7 mmol) was added last, and the mixture was heated to 95 °C for 20 h. The reaction was concentrated under reduced pressure, combined with pentane (300 mL), and filtered through a Celite pad. The filtrate was washed with distilled water, and the organic phase was dried with $MgSO_4$ and filtered. The solvent was removed by rotary evaporation to afford 2.615 g (98%) of a crystalline yellow solid. ^{1}H NMR ($CDCl_3$): 7.17 (d, 2H, J = 5 Hz), 7.06 (d, 2H, J = 5 Hz), 0.25 (s, 18H) ppm. ^{13}C NMR ($CDCl_3$): δ 139.0, 130.6, 123.8, 119.3, 101.5, 100.7, −0.4 ppm. MS (EI): m/z 358 (M^+, 36%), 73 [$(M - C_{15}H_{13}S_2Si)^+$, 100%]. FT-IR (KBr): 3087 (w), 2954 (m), 2897 (w), 2147 (s), 1493 (w), 1359 (w), 1239 (m), 1081 (w), 950 (m), 886 (m), 844 (s), 756 (m), 712 (s), 634 (m), 433 (w) cm^{-1}. Calcd for (found %) $C_{12}H_{14}O_2Si$ = C: 60.32 (59.96), H: 6.20% (6.19).

3,3′-Diethynyl-2,2′-bithiophene (2). **1** (1.000 g, 2.79 mmol) was dissolved in a deaerated mixture of dry tetrahydrofuran (THF) and EtOH (100 mL). Potassium hydroxide (0.328 g, 5.860 mmol) was added to the solution. The reaction mixture was stirred at room temperature overnight, H_2O (20 mL) was added, and the solvent was concentrated under reduced pressure. The residue was dissolved in CH_2Cl_2 and washed with distilled water (300 mL). The organic phase was dried over $MgSO_4$, filtered, and the solvent was removed by rotary evaporation to obtain a brown oil that was sufficiently pure to proceed immediately with the next step. ^{1}H NMR ($CDCl_3$): δ 7.23 (d, 1H, J = 5 Hz), 7.12 (d, 1H, J = 5 Hz), 3.35 (s, 1H) ppm. HRMS (EI +) calculated for $[C_{12}H_6S_2]^+$: 213.99110 found 213.99102.

(30) Choi-Sledeski, Y. M.; McGarry, D. G.; Green, D. M.; Mason, H. J.; Becker, M. R.; Davis, R. S.; Ewing, W. R.; Dankulich, W. P.; Manetta, V. E.; Morris, R. L.; Spada, A. P.; Cheney, D. L.; Brown, K. D.; Colussi, D. J.; Chu, V.; Heran, C. L.; Morgan, S. R.; Bentley, R. G.; Leadley, R. J.; Maignan, S.; Guilloteau, J.-P.; Dunwiddie, C. T.; Pauls, H. W. *J. Med. Chem.* **1999**, *42*, 3572–3587.

5-Iodosalicylaldehyde (3). The following procedure is a modified version of Pauls and co-workers.[30] A 1.0 M solution of iodine monochloride in dry THF (100 mL) was added to a flask containing a mixture of salicylaldehyde (12.2 g, 0.100 mol) and I_2 (25.38 g, 0.100 mol). The reaction was stirred at room temperature for 48 h, and then added to a saturated aqueous solution of Na_2SO_3 (1 L). The solution was stirred at room temperature as the purple color gradually disappeared, and the THF was completely evaporated resulting in a precipitate that was filtered, washed with water, and dried providing 23.3 g (94%) of a white solid. ^{1}H NMR ($CDCl_3$): δ 10.97 (br s, 1H), 9.85 (s, 1H), 7.87 (d, 1H, J = 2 Hz), 7.80 (dd, 1H, J = 9, 2 Hz), 6.83 (d, 1H, J = 9 Hz), ppm. MS (EI): m/z 248 (M^+, 100%).

3,3′-Bis(5-ethynylsalicylaldehyde)-2,2′-bithophene (4). **2** (0.597 g, 2.79 mmol), **3** (1.522 g, 6.14 mmol), PPh_3 (0.073 g, 10 mol %), $Pd(PPh_3)_2Cl_2$ (0.196 g, 10 mol %), and CuI (0.053 g, 10 mol %) were added to anhydrous and deareated THF (100 mL) containing diisopropylamine (0.9 mL). The reaction was stirred at 43 °C for 20 h, cooled to room temperature, and concentrated under reduced pressure. The residue was combined with $CHCl_3$ (100 mL), filtered through a Celite pad with CH_2Cl_2 (400 mL), and washed with 0.5 M HCl (400 mL). The organic phase was dried over $MgSO_4$, filtered, and the solvent was removed by rotary evaporation. The solution was concentrated (25 mL) and added dropwise to pentane (500 mL), resulting in a precipitate that was collected by vacuum filtration. The precipitate was washed with pentane (25 mL), ice cold methanol (15 mL), and dried to afford 1.84 g (77%) of yellow powder. ^{1}H NMR ($CDCl_3$): δ 11.13 (br s, 2H), 9.89 (s, 2H), 7.77 (d, 2H, J = 2 Hz), 7.72 (dd, 2H, J = 9, 2 Hz), 7.28 (d, 2H, J = 5 Hz), 7.26 (d, 2H, J = 5 Hz), 7.01 (d, 2H, J = 9 Hz) ppm. ^{13}C NMR ($CDCl_3$): δ 196.1, 161.6, 139.5, 138.1, 136.7, 130.4, 124.4, 120.6, 119.2, 118.3, 115.3, 93.6, 85.2 ppm. HRMS (EI +) calculated for $[C_{26}H_{14}O_4S_2]^+$: 454.03335 found 454.03347. FT-IR (KBr): 3424 (w). 3080 (w), 2924 (w), 2852 (w), 1655 (s), 1614 (w), 1580 (w), 1503 (m), 1476 (m), 1372 (w), 1282 (m), 1261 (m), 1222 (w), 1186 (w), 1137 (w), 906 (w), 879 (w), 844 (w), 766 (w), 723 (w), 705 (w), 684 (w), 636 (w) cm^{-1}. Calcd for (found %) $C_{26}H_{14}O_4S_2.H_2O$ = C: 66.10 (65.94), H: 3.42% (3.38).

BT(QsalH)$_2$ (5). **4** (0.150 g, 0.330 mmol) was dissolved in a THF (15 mL) and added to a solution of 8-aminoquinoline (0.185 g, 1.29 mmol) in ethanol (15 mL). The solution was deaerated and stirred at room temperature for 24 h. The mixture was then concentrated under reduced pressure and dissolved in $CHCl_3$ (1.0 mL) and precipitated into warm hexane (15 mL). The solid was collected by vacuum filtration, washed with hexanes, and dried to give 0.166 g (71%) of an orange solid. ^{1}H NMR ($CDCl_3$): δ 14.66 (br s, 2H), 9.21 (s, 2H), 9.01 (d, 2H, J = 3 Hz), 8.48 (dd, 2H, J = 8.5, 1.5 Hz), 7.98 (m, 4H), 7.85 (d, 2H, J = 7 Hz), 7.75 (m, 8H), 7.31 (d, 2H, J = 5 Hz), 7.08 (d, 2H, J = 8.5 Hz) ppm. The instability of **5** in solution over even short periods of time precluded the acquisition of a publishable ^{13}C NMR spectrum. HRMS (FAB +) calculated for $[C_{44}H_{27}O_2N_4S_2]^+$: 707.15755 found 707.13532. FT-IR (KBr): 3449 (w), 3096 (w), 2925 (w), 2853 (w), 1620 (s), 1482 (w), 1385 (w), 1285 (w), 1121 (w), 1083 (w), 886 (w), 826 (w), 792 (w), 716 (w),

635 (w), 595 (w) cm^{-1}. Calcd for (found %) $C_{44}H_{26}O_2N_4S_2$ = C: 74.77 (74.50), H: 3.71 (3.62), N: 7.93% (7.69).

{(5)[Fe(Qsal)$_2$]$_2$}Cl$_2$ (6). **4** (0.681 g, 1.50 mmol) was dissolved in deaerated THF (30 mL), combined with 8-aminoquinoline (0.432 g, 3.00 mmol), and stirred for 24 h. $FeCl_3 \cdot 6H_2O$ (0.810 g, 3.00 mmol) was added to the mixture, and the solution was stirred for 2 h. The resulting precipitate was washed with water, pentane, dried and suspended in MeOH (20 mL). 8-aminoquinoline (0.389 g, 2.70 mmol) and salicylaldehyde (0.329 g, 2.70 mmol) in MeOH (10 mL) were added to the suspension. The mixture was stirred overnight, washed with water, pentane, and dried, affording 1.615 g (78%) of brown powder. MS (MALDI +): m/z 1310 [(M − 2Cl)$^+$], 1063 [(M − Qsal + 2Cl)$^+$], 550 [(Fe(Qsal)$_2$)$^+$], 303 [(Fe(Qsal)$^+$]. Calcd for (found %) $C_{76}H_{46}N_8O_4S_2Fe_2Cl_2$ = C: 65.83 (66.04), H: 2.99 (3.36), N: 8.00% (8.11). FT-IR (KBr): 3421 (w), 3049 (w), 2924 (w), 2856 (w), 2191 (w), 1603 (s), 1574 (s), 1525 (s), 1504 (s), 1456 (m), 1396 (w), 1375 (m), 1307 (m), 1240 (w), 1194 (w), 1147 (w), 1130 (w), 1086 (w), 972 (w), 930 (w), 883 (w), 829 (m), 760 (w), 708 (w), 633 (w), 542 (w), 511 (m), 457 (w) cm^{-1}.

{(5)[Fe(Qsal)$_2$]$_2$}(SCN)$_2$ (7) and {(5)[Fe(Qsal)$_2$]$_2$}(PF$_6$)$_2$ (8). **6** (0.150 g, 0.109 mmol) was suspended in MeOH (30 mL), and an excess of $NaPF_6$ **8** (0.073 g, 0.434 mmol), or KSCN **7** (0.042 g, 0.434 mmol), was added. The mixture was stirred overnight and then combined with distilled water (250 mL), which resulted in brown precipitates that were filtered off, washed with water, pentane, and dried. {**(5)[Fe(Qsal)$_2$]$_2$}(SCN)$_2$**$\cdot$2KCl (7). Yield 0.132 g (85%). MS (FAB+): m/z 1368 [M − SCN]$^+$, 1310 [M − 2SCN]$^+$, 1063 [M − (2SCN + Qsal)]$^+$, 550 [Fe(Qsal)$_2$$^+$], 307 [Fe(Qsal)$^+$]. Calcd for (found %) $C_{78}H_{46}N_{10}O_4S_4Fe_2 \cdot 2KCl$ = C: 60.49 (60.49), H: 3.25 (2.96), N: 7.24% (7.99). FT-IR (KBr): 3410 (w), 3051 (w), 2924 (w), 2852 (w), 2195(w), 2038 (s), 1602 (s), 1574 (s), 1525 (s), 1504 (s), 1458 (s), 1429 (w), 1396 (w), 1377 (m), 1308 (m), 1240 (w), 1194 (w), 1147 (w), 1068 (w), 972 (w), 931 (w), 883 (w), 829 (m), 785 (w), 758 (w), 719 (w), 634 (w), 542 (w), 511 (w), 463 (w), 414 (w) cm^{-1}. {**(5)[Fe(Qsal)$_2$]$_2$}(PF$_6$)$_2$ (8).** Yield 0.155 g (89%). MS (FAB+): m/z 1310 [M − 2PF$_6$]$^+$, 1063 [M − (2PF$_6$ + Qsal)]$^+$, 550 [Fe(Qsal)$_2$$^+$], 307 [Fe(Qsal)$^+$]. Calcd for (found %) $C_{76}H_{46}N_8O_4S_2Fe_2P_2F_{12}$ = C: 57.00 (57.34), H: 2.90 (2.66), N: 7.00% (6.69). FT-IR (KBr): 3419 (w), 3066 (w), 2924 (w), 2852 (w), 2193 (w), 1604 (s), 1576 (s), 1525 (s), 1504 (s), 1458 (s), 1398 (w), 1377 (m), 1309 (m), 1242 (w), 1194 (w), 1149 (w), 1088 (w), 972 (w), 931 (w), 843 (s), 787 (w), 760 (w), 721 (w), 634 (w), 557 (m), 512 (w), 463 (w) cm^{-1}.

{(5)[Fe(Qsal)$_2$]$_2$}(ClO$_4$)$_2$ (9). **6** (0.274 g, 0.604 mmol) was dissolved in deaerated THF (60 mL), combined with 8-aminoquinoline (0.174 g, 1.207 mmol), and stirred for 24 h. $Fe(ClO_4)_2 \cdot 6H_2O$ (429 g, 1.207 mmol) was added, and the solution was stirred for 2 h. The resulting precipitate was washed with water, pentane, dried, and then suspended in MeOH (30 L). 8-aminoquinoline (0.115 g, 0.799 mmol) and salicylaldehyde (0.097 g, 0.799 mmol) in MeOH (10 mL) were added to the suspension. The mixture was stirred overnight, washed with water, pentane, and dried to give 0.358 g (39%) of brown powder. MS (MALDI+): m/z 1410 [M − ClO$_4$]$^+$, 1008 [M − (Fe + Qsal + 2ClO$_4$)]$^+$, 550 [Fe(Qsal)$_2$$^+$], 303 [Fe(Qsal)$^+$]. Calcd for (found %) $C_{76}H_{46}N_8O_{12}S_2Fe_2Cl_2$ = C: 60.44 (60.30), H: 3.07 (2.91), N: 7.42% (7.10). FT-IR (KBr): 3447 (br w), 3071 (w), 2923 (w), 2851 (w), 2195 (w), 1603 (s), 1574 (s), 1525 (s), 1505 (s), 1457 (s), 1397 (m), 1378 (m), 1308 (m), 1242 (w), 1194 (w), 1089 (s), 973 (w), 884 (w), 832 (m), 790 (w), 760 (w), 729 (w), 622 (m), 547 (w), 512 (w), 460 (w), 415 (w) cm^{-1}.

Scheme 1. Preparation of **1**−**9**[a]

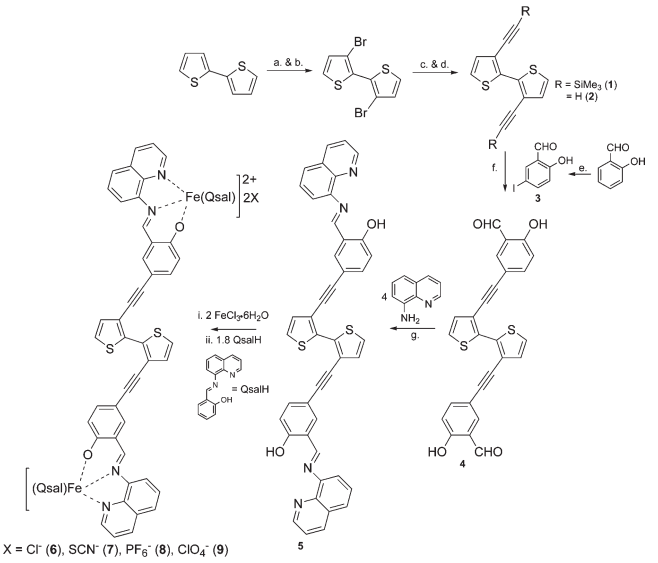

[a] Reagents and conditions; (a) 48% HBr(aq) and Br_2/HOAc; (b) Zn dust, HCl/HOAc; (c) 3 equiv of ethynyltrimethylsilane, 6 mol % Pd$(PPh_3)_2Cl_2$, 6 mol % PPh_3, 6 mol % CuI, $^iPr_2NH$, 95 °C, 20 h; (d) 2.1 equiv of KOH, THF/EtOH, 24 h, RT; (e) 1 equiv of ICl (1.0 M THF), 1 equiv of I_2, 48 h, RT; (f) **2**, 10 mol % Pd$(PPh_3)_2Cl_2$, 10 mol % PPh_3, 10 mol % CuI, THF, $^iPr_2NH$, 43 °C, 20 h; (g) THF/EtOH, 24 h, RT.

Results and Discussion

Ligand Synthesis, Coordination Chemistry, and Structural Studies. Bridging ligand **5** was prepared in six steps from commercially available 2,2′-bithiophene (Scheme 1). 3,3′-Dibromo-2,2′-bithiophene was obtained via a literature bromination of 2,2′-bithiophene to generate 3,3′-5,5′-tetrabromo-2,2′-bithiophene, followed by reductive dehalogenation with zinc metal to produce the dibrominated product.[31] Sonogashira methodology using ethynyltrimethylsilane provided **1**, which was deprotected with KOH to the rather unstable 3,3′-diethynyl-2,2′-bithiophene **2**. We found the best results were obtained when using **2** in the next step, directly following a quick purification step and routine characterization.

Our first attempts to generate dialdehyde **4** included Sonogashira reactions between **2** with commercially available 5-bromosalicylaldehyde; however, these reactions did not provide reasonable yields of the dialdehyde product. Next, we turned our attention to 5-iodosalicylaldehyde **3**, which was generated easily from salicylaldehyde, iodine, and iodine monochloride, using a modified literature procedure.[30] Sonogashira reaction between **2** with 2.2 equiv of 5-iodosalicylaldehyde at ∼45 °C afforded dialdehyde **4**, reproducibly and in good yield. The X-ray crystal structure of **4** was determined and an Oak

(31) Yu, W.-L.; Meng, H.; Pei, J.; Huang, W.; Li, Y.; Heeger, A. J. *Macromolecules* **1998**, *31*, 4838–4844.

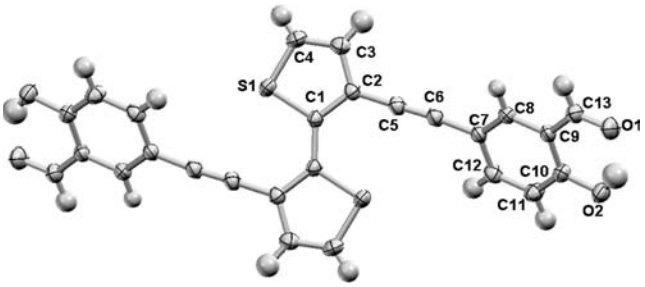

Figure 2. Molecular structure of **4** (thermal ellipsoids at 50%).

Ridge Thermal Ellipsoid Plot (ORTEP) diagram of the molecular structure of **4** is shown in Figure 2. Structural details and a table of relevant bond lengths and angles are provided in Tables 1 and 2, respectively.

Ligand **5** was isolated by reaction of **4** with 4 equiv of 8-aminoquinoline, to produce an orange, analytically pure solid, following purification. Using less than 4 equiv of 8-aminoquinoline resulted in an incomplete conversion to the diimine. This material is unstable in solution and over short periods of time while stored as a solid, but was fully characterized, and features a hydroxyl proton resonance at 14.7 ppm in the ^{1}H NMR spectrum. The C=N imine absorption in the FTIR spectrum is observed at 1620 cm^{-1}. Because of the instability of **5** we found it was best to prepare it in situ prior to metal coordination, rather than store the solid.

Bimetallic iron(3+) complex **6**, containing two Cl^- counteranions, was prepared by reaction of 2 equiv of $FeCl_3 \cdot 6H_2O$ with **5** (generated in situ) followed by addition of slightly less than 2 equiv of QsalH to "cap" the available coordination sites on the iron centers, to produce an analytically pure powder that served as the starting point for the preparation of complexes **7** and **8**. When we attempted to generate bimetallic complexes in one step, by combining **5** with an iron(3+) salt and 2 equiv of QsalH, we isolated a significant amount of $Fe(Qsal)_2^+$ with very little bimetallic product, and so our stepwise coordination was necessary. Complexes **7** and **8**, containing SCN^- and PF_6^- counteranions, respectively, were generated by metathesis of **6** with aqueous solutions containing an excess of KSCN or $NaPF_6$. Perchlorate analogue **9** was prepared by reacting **5** with $Fe(ClO_4)_3 \cdot 9H_2O$ directly, followed by addition of 2 equiv of QsalH. Complexes **6**−**9** are analytically pure powders, provide characteristic FAB or MALDI-TOF mass spectra (Supporting Information, Figures S1−S4), and feature very similar FTIR spectra (Supporting Information, Figures S5−S8), including a $\nu_{C=N}$ absorption at ∼1604 to 1602 cm^{-1}, which is shifted to lower energy than the same absorption in uncoordinated **5**. The only differences in the FTIR spectra of **6**−**9** result from the particular absorptions of the different counteranions. Unfortunately single crystals suitable for X-ray diffraction could not be obtained for any of **6**−**9** using a variety of crystallization techniques (including slow evaporation and solvent diffusion with H-tubes), which are insoluble in any nonpolar solvents and very poorly soluble in all polar solvents that we tried. That said, based on all of our analytical and spectroscopic data, we are confident in the reported assigned structures and purity of the precipitated powders.

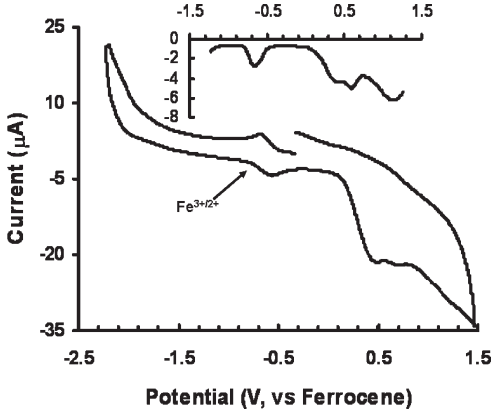

Figure 3. Cyclic voltammogram of **7** recorded in deaerated CH_3CN solution containing 0.1 M NEt_4PF_6. Inset: Differential pulse voltammogram of **7** [conditions identical to those for CV experiment; *x*-axis is potential (V) versus ferrocene, and *y*-axis is current in μA].

Table 1. Crystallographic Data for **4**

formula	$C_{26}H_{14}O_4S_2$
fw	454.49
dimensions (mm)	0.60 × 0.20 × 0.06
a (Å)	16.404(2)
b (Å)	11.7203(16)
c (Å)	12.1821(17)
cryst syst	monoclinic
α (deg)	90
β (deg)	116.637(3)
γ (deg)	90
volume (Å^3)	2093.48(5)
space group	$C_{2/c}$
Z	4
μ (mm^{-1})	0.287
T (K)	295(2)
independent reflections	2174, R_{int} = 0.0283
number of parameters	173
R_1 [$F^2 > 2\sigma(F^2)$]	0.0396
$wR_2(F^2)^a$	0.116

$^a w = 1/[\sigma^2(F_o^2) + (0.069P)^2 + 0.2902P]$ where $P = (F_o^2 + 2F_c^2)/3$.

Table 2. Selected Bond Distances (Å) and Selected Bond Angles (deg) for **4**

bond	(Å)	angle	(deg)
S1−C4	1.709(2)	C4−S1−C1	92.14(10)
S1−C1	1.7317(18)	C2−C1−C1′	129.0(2)
O1−C13	1.223(3)	C2−C1−S1	109.88(13)
O2−C10	1.348(2)	C1−C2−C3	112.23(17)
C1−C2	1.396(3)	C1−C2−C5	125.05(17)
C1−C1′	1.454(3)	C3−C2−C5	122.72(17)
C2−C3	1.424(3)	C3−C4−S1	112.61(18)
C2−C5	1.429(3)	C6−C5−C2	178. 6(2)
C3−C4	1.337(3)	C5−C6−C7	173.9(2)
C5−C6	1.201(3)	O2−C10−C11	118.60(18)
C6−C7	1.431(3)	O2−C10−C9	122.07(17)
		O1−C13−C9	124.4(2)

Electrochemical Properties. The electrochemical properties of complexes **6**−**9** have been investigated using cyclic voltammetry (CV) and differential pulse voltammetry (DPV). The electrochemical results are very similar to those observed for the reported monometallic iron(3+) complexes of the thienyl-substituted Qsal ligand.[29] As an example, the CV and DPV acquired from an acetonitrile solution of **7** is shown in Figure 3, and the other electrochemical data for compounds **5**, and **6**, **8**, and **9**, which are very similar to **7**, are found in the Supporting Information, Figures S9−S12. Toward anodic potentials

(versus ferrocene), complexes **6**−**9** feature broad and irreversible oxidation waves centered at potentials of +0.3 and +1.1 V. Deconvolution by DPV suggests that there are at least three distinct anodic processes in **7** at +0.4, +0.6, and +1.1 V (these potentials are a little more or less positive for **6**, **8**, and **9**). These waves are also present in the CV of the uncoordinated ligand **5**, and so are ascribed to irreversible ligand centered oxidations in the metal complexes. In particular, the most positive oxidation in all cases likely results from oxidation of the 2,2′-bithienyl bridge. We observed similar potentials for the oxidation of thienyl-substituted Qsal ligands, previously.[29] We also note that **5** features another irreversible oxidation centered at +0.2 V, which is not observed in the CV of **6**−**9**, and likely results from hydroxyl group oxidation. Also, because of the instability of **5** in solution, it is possible that some of the observed waves in the CV and DPV of this compound could have originated from decomposition products. Electrochemical results for **5**−**9** can be found in Table 3.

Over cathodic potentials, one pseudo-reversible wave, representing iron(3+) reduction, is observed and is centered at potentials of −0.6 or −0.7 V for each of **6**−**9**. No evidence for redox splitting of the iron(3+) reduction wave is observed (including at different scan rates from 10 to 200 mV/s), suggesting very little, if any, electronic communication between metal centers in the complexes, which is anticipated based on the rather long distance that is expected between metal centers. At very negative potentials (> −2.0 V), broad irreversible processes are observed, which are likely due to imine bond reduction.

We attempted to electrochemically polymerize complexes **6**−**9** by repeated scans over the 2,2′-bithienyl oxidation potentials; however, in all cases no polymerization was observed (neither current increases with increasing scan number nor deposited electroactive films on the working electrode were observed). Poor monomer solubility, steric congestion, and the high irreversible 2,2′-bithienyl oxidation potential all likely contribute to the inability of **6**−**9** to polymerize. We are actively pursing other QsalH derivatives featuring substituents (for example, terthienyl and ethylenedioxythiophene), which we anticipate will be much more amenable to electropolymerization reactions.

Variable Temperature Magnetic Susceptibility, Mössbauer and EPR Spectroscopy. Evidence for temperature dependent spin-crossover behavior for complexes **6**−**8** (the data for **9**, which is different from the data obtained for **6**−**8**, is discussed later) is provided by variable temperature magnetic susceptibility measurements recorded on analytically pure powdered samples using a SQUID magnetometer (temperature range 2−350 K). The data are displayed as plots of $\chi_M T$ versus T in Figure 4. For each complex a very gradual decrease in $\chi_M T$ with decreasing temperature toward 20 K is noted, followed by a more rapid decrease below 20 to 2 K, and no hysteresis is observed upon warming from 2 K back to 350 K, which is typical behavior for iron(3+) spin-crossover systems. The $\chi_M T$ values at 350 K for **6**−**8** are a little less than the anticipated values for two high-spin (S = 5/2) iron(3+) ions in the absence of any magnetic coupling (theoretical spin-only value is 8.75 cm^3 K mol^{-1}). We assert that the lower $\chi_M T$ values that we observe at 350 K result from some proportion of the lower-spin isomer present at this temperature and are not the result of any intramolecular antiferromagnetic coupling. This claim is supported both by our electrochemical results, which suggest no electronic coupling between the iron(3+) ions at room temperature, and the results from Mössbauer spectroscopy (vide infra). At the lowest measured temperature (2 K), $\chi_M T$ values for **6**−**8** suggest a lower spin state but not the expected S = 1/2 for each iron (3+) atom in the lowest spin state (theoretical value is 0.75 cm^3 K mol^{-1}). Rather, the $\chi_M T$ values observed at 2 K (approximately 3.5 cm^3 K mol^{-1}) suggest a mixture of nearly 35% S = 5/2, 5/2 and 65% S = 1/2, 1/2 iron (3+), indicating an incomplete spin-crossover for each of **6**−**8**. To help with our interpretation of the data from variable temperature magnetic susceptibility studies, we have also obtained Mössbauer spectra for complexes **6**−**9** at 293, 200, 100, and 6 K. The data are plotted for each complex (Figure 5), and Mössbauer parameters for all complexes are listed in Table 4. Similar to the magnetic data, complexes **6**−**8** share similar Mössbauer properties, while **9** is rather different. In all cases, the Mössbauer data indicate the presence of two different sets of spin states in thermal equilibrium with one another. For **6**−**8**, Mössbauer spectra at 293 K are very similar, and each spectrum displays a doublet with quadrupole splittings (> 0.9 mm/s) and isomer shifts (> 0.3 mm/s) that are typical for other reported monometallic high-spin iron(3+) bis-Qsal complexes, and another smaller component, with Mössbauer parameters that suggest an S = 1/2, 1/2 state.[32−34] With decreasing temperature,

Table 3. Electrochemical Data for Compounds **5**−**9**[a]

compound	E'_{ox} (V)	E'_{red} (V)
5	+0.2, +0.6, +0.9, +1.2	−0.7, −2.1, −2.3
6	+0.3, +0.8, +1.1	−0.6
7	+0.4, +0.6, +1.1	−0.6
8	+0.4, +0.9, +1.1	−0.7
9	+0.5, +1.1	−0.6

[a] All experiments were performed in CH_3CN, containing 0.1 M $^nEt_4NPF_6$ supporting electrolyte, and all potentials are quoted versus ferrocene/ferrocenium reference.

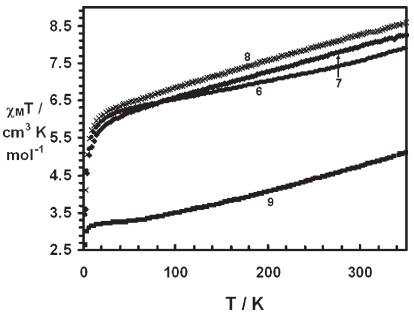

Figure 4. Temperature dependence of $\chi_M T$ values **6** (●), **7** (♦), **8** (×), and **9** (■) (5000 Oe field).

(32) Faulman, C.; Dorbes, S.; Lampert, S.; Jacob, K.; Garreau de Bonneval, B.; Molnar, G.; Bousseksou, A.; Real, J. A.; Valade, L. *Inorg. Chim. Acta* **2007**, *360*, 3870–3878.
(33) Takahashi, K.; Cui, H.-B.; Okano, Y.; Kobayashi, H.; Mori, H.; Tajima, H.; Einaga, Y.; Sato, O. *J. Am. Chem. Soc.* **2008**, *130*, 6688–6689.
(34) Dickinson, R. C.; Baker, W. A.Jr.; Collins, R. L. *J. Inorg. Nucl. Chem.* **1977**, *39*, 1531–1533.

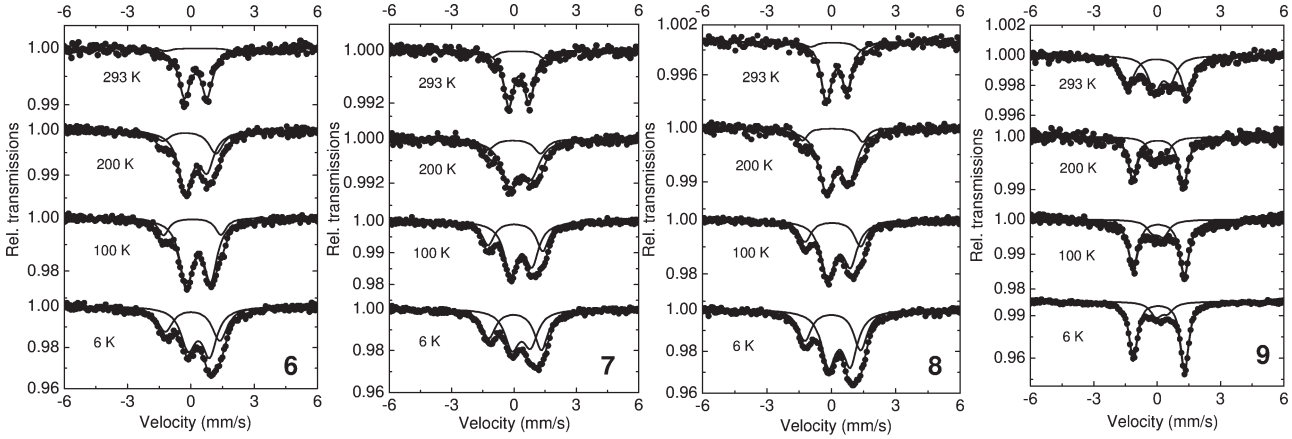

Figure 5. Temperature dependent Mössbauer spectra for **6**−**9** (the top spectra were measured at 293 K, and the spectra beneath at 200, 100, and 6 K, respectively). The dots represent the observed spectra; lines indicate simulated high-spin, low-spin, and the sum of high- and low-spin curves.

Table 4. Mössbauer Data for **6**−**9**[a]

T (K)	compound	IS (mm/s)	QS (mm/s)	site (%)	spin state
293	**6**	0.34(1)	1.07(1)	95	5/2, 5/2
		0.40(9)	3.2(4)	5	1/2, 1/2
	7	0.35(1)	0.92(2)	88	5/2, 5/2
		0.31(7)	2.6(1)	12	1/2, 1/2
	8	0.36(1)	0.96(2)	87	5/2, 5/2
		0.30(9)	2.4(1)	13	1/2, 1/2
	9	0.26(2)	0.76(3)	45	5/2, 5/2
		0.13(1)	2.78(2)	56	1/2, 1/2
200	**6**	0.34(1)	0.96(2)	74	5/2, 5/2
		0.07(2)	2.48(3)	26	1/2, 1/2
	7	0.43(3)	1.03(5)	80	5/2, 5/2
		0.11(4)	2.54(1)	20	1/2, 1/2
	8	0.36(1)	0.93(2)	72	5/2, 5/2
		0.11(2)	2.53(4)	28	1/2, 1/2
	9	0.25(3)	0.58(5)	30	5/2, 5/2
		0.16(1)	2.39(3)	70	1/2, 1/2
100	**6**	0.44(1)	1.08(1)	72	5/2, 5/2
		0.14(1)	2.58(3)	28	1/2, 1/2
	7	0.47(1)	1.05(2)	69	5/2, 5/2
		0.18(1)	2.65(3)	31	1/2, 1/2
	8	0.43(1)	0.98(1)	62	5/2, 5/2
		0.14(1)	2.57(2)	38	1/2, 1/2
	9	0.16(4)	0.51(5)	23	5/2, 5/2
		0.19(1)	2.42(1)	77	1/2, 1/2
6	**6**	0.49(1)	1.01(5)	58	5/2, 5/2
		0.19(1)	2.59(5)	42	1/2, 1/2
	7	0.47(2)	0.91(3)	54	5/2, 5/2
		0.17(1)	2.55(2)	46	1/2, 1/2
	8	0.47(1)	0.96(1)	57	5/2, 5/2
		0.17(1)	2.58(1)	43	1/2, 1/2
	9	0.33(2)	0.55(2)	20	5/2, 5/2
		0.20(1)	2.43(2)	80	1/2, 1/2

[a] The numbers in parentheses are error bars obtained from the theoretical fittings to the experimental data.

a decrease in the intensity of the high-spin doublet is noted, accompanied by an intensity increase in the low-spin doublet. The changes in the proportion of each state are small and occur very slowly, which is also reflected in the variable temperature magnetic data. For instance, at 6 K the Mössbauer spectrum of **6** indicates 58% high-spin and 42% low-spin components. The value of $\chi_M T$ at this temperature (5.2 cm^3 K mol^{-1}) is very similar to the theoretical value (5.39 cm^3 K mol^{-1}) for the proportion of spin isomers observed from the Mössbauer spectrum. Taken together, our variable temperature susceptibility and Mössbauer data suggest that nearly, but not exactly, half of the iron(3+) in **6**−**8** at very low temperature is in the high-spin state, and the possible molecular interpretation of these observations is twofold: Half of the molecules feature $S = 5/2, 5/2$ or $S = 1/2, 1/2$, iron(3+); alternatively, each particular molecule has one high-spin and one low-spin iron(3+) ion ($S = 5/2, 1/2$). To know conclusively the correct interpretation, we would need to look at the X-ray crystal structure of each complex at low temperature and compare coordinate bond lengths. In the absence of this data, because of the solubility limitations discussed previously, we are unable at this time to ascertain which interpretation is correct. On the basis of data from other reported bimetallic iron(3+) SCO complexes for which X-ray structures are known, it is much more common to observe HS-HS to LS-LS crossovers, without accessing an intermediate HS-LS state.

The variable temperature magnetic susceptibility data for complex **9** are significantly different from the profiles observed for **6**−**8**. At 350 K, $\chi_M T$ is 5.1 cm^3 K mol^{-1} and suggests a considerably larger component of the low iron (3+) spin states at this temperature, which is also supported by the high temperature Mössbauer spectrum of **9**. Mössbauer data at 293 K suggest a larger component of the low-spin isomer at this temperature (55%), and this is also mirrored in the magnetic susceptibility data at the same temperature. At 293 K, the value of $\chi_M T$ is 4.7 cm^3 K mol^{-1}, which is very close to the anticipated value (4.32 cm^3 K mol^{-1}) for a mixture of $S = 5/2, 5/2$ and $S = 1/2, 1/2$ isomers in a proportion defined by the Mössbauer spectrum. As temperature decreases, the doublet associated with the $S = 1/2, 1/2$ state increases in intensity, and the $S = 5/2, 5/2$ doublet decreases. At 6 K, the Mössbauer spectrum of **9** indicates 20% $S = 5/2, 5/2$ and 80% $S = 1/2, 1/2$, which is supported by the value of $\chi_M T$ (3.1 cm^3 K mol^{-1}) at 6 K that is close to the expected value (2.4 cm^3 K mol^{-1}) calculated for the proportion of spin isomers from the 6 K Mössbauer spectrum. The different magnetic properties observed from **9** likely have their origins in different structural properties compared with **6**−**8**. In fact, completely high-spin and low-spin $Fe(Qsal)_2^+$ complexes have been observed, each containing an identical cation, but differing only in counteranion (Cl or I), so the observations reported herein are not unprecedented.[34]

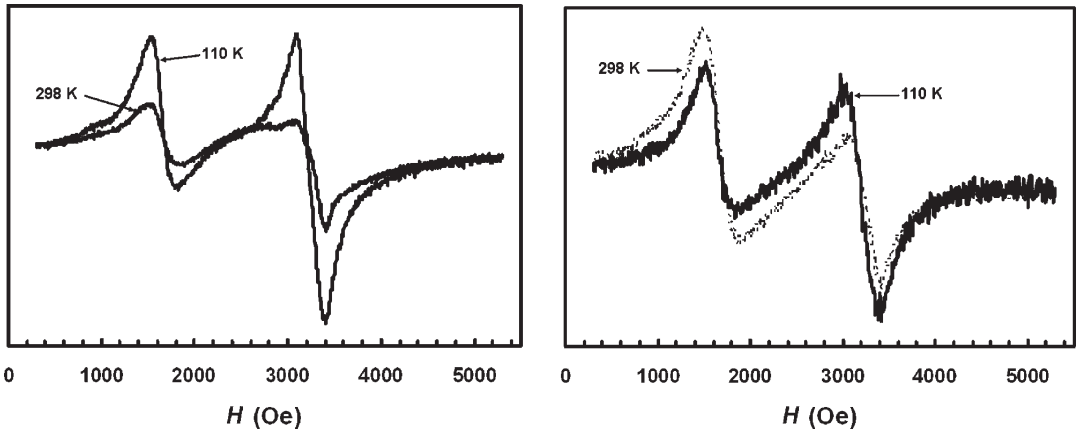

Figure 6. Powder EPR spectra of **8** (left) and **9** (right) at 298 and 110 K.

Powder EPR spectra were obtained from samples of each complex at 298 and 110 K, and the data for **8** and **9** are shown in Figure 6 (spectra for **6** and **7** are provided in the Supporting Information, Figures S13 and S14). For complexes **6**, **7**, and **8** nearly identical spectra are obtained at each temperature, once more reflecting the similar magnetic properties exhibited by these complexes. The room temperature spectrum indicates the presence of both $S = 5/2$ ($g = 4.3$) and $S = 1/2$ ($g = 2.1$) iron(3+), with rhombic symmetry and broad resonances. With decreasing temperature (110 K), the resonances become slightly more resolved and intense, and provide *g*-values that are similar to those observed in the room temperature spectrum, indicating that a significant proportion of $S = 5/2, 5/2$ and $S = 1/2, 1/2$ complexes are present at this temperature, which is supported by the Mössbauer and magnetic susceptibility data. The broadness of the resonances is attributed to spin−spin interactions, which has been observed for other iron(3+) spin-crossover complexes.[35,36] Complex **9** exhibits nearly identical EPR spectra at each temperature, with only small intensity differences, which result from the small decrease in the proportion of the high-spin isomer between these temperatures.

Conclusions

Compared with the number of reported bimetallic iron(2+) SCO complexes, reports of similar bimetallic iron(3+) analogues are exceptionally rare. We reasoned that a 2,2′-bithienyl substituent would make a nice scaffold for constructing bimetallic $Fe(Qsal)_2^+$ complexes, and four bimetallic iron(3+) spin-crossover complexes of a new 2,2′-bithienyl-bridging bis-QsalH ligand are reported in the present work. In each complex, SCO is very gradual and incomplete, as indicated by data from variable temperature magnetic susceptibility, Mössbauer, and EPR spectroscopy. Of interest, ClO_4 complex **9** featured magnetic properties that were rather different from the other complexes, which likely originate from different structural properties between complexes **6**−**8** and **9**. To enhance the solubility of these materials so that better structural data can be obtained, we are currently preparing analogues of bridging ligand **5** containing solubilizing substituents on the 2,2′-bithienyl substituent. We are also pursuing other ligand structural types that will bring the iron(3+) ions closer together to perhaps enhance electronic or magnetic coupling and generate multifunctional bimetallic iron(3+) analogues to known exchange-coupled bimetallic iron(2+) SCO complexes. Work in this regard is underway and will be reported in due course.

Acknowledgment. The authors acknowledge financial support from the Natural Sciences and Engineering Research Council of Canada. M.T.L. thanks Brock University for providing start-up funds, and NSERC (Discovery and RTI).

Supporting Information Available: FT-IR and FAB or MALDI-TOF mass spectra of **6**−**9**, cyclic voltammograms for **5**, **6**, **8**, and **9**, EPR data for **6**−**7** and crystallographic data in CIF format. This material is available free of charge via the Internet at http://pubs.acs.org.

(35) Simaan, A. J.; Boillot, M.-L.; Rivière, E.; Boussac, A.; Girerd, J.-J. *Angew. Chem., Int. Ed.* **2000**, *39*, 196–198.
(36) Tang, J.; Costa, J. S.; Smulders, S.; Molnár, G.; Bousseksou, A.; Teat, S. J.; Li, Y.; van Albada, G. A.; Gamez, P.; Reedijk, J. *Inorg. Chem.* **2009**, *48*, 2128–2135.